Implantable wireless transmission rectenna system for biomedical wireless applications

Shuoliang Ding, Stavros Koulouridis, Lionel Pichon

▶ To cite this version:

HAL Id: hal-02976880
https://hal.science/hal-02976880

Submitted on 6 Nov 2020

IEEE *Access*

Implantable Wireless Transmission Rectenna System for Biomedical Wireless Applications

SHUOLIANG DING[1], **STAVROS KOULOURIDIS**[2], **AND LIONEL PICHON**[1]

[1]CentraleSupélec, CNRS, Group of Electrical Engineering-Paris, University of Paris-Saclay, 91192 Gif-sur-Yvette, France
[2]Electrical and Computer Engineering Department, University of Patras, 265 04 Patras, Greece

Corresponding author: Shuoliang Ding (shuoliang.ding@geeps.centralesupelec.fr)

ABSTRACT We introduce a novel RF to DC wireless power transmission implantable rectenna system at Industrial, Scientific and Medical bands (ISM 902.8-928 MHz). An embedded circular antenna receives the externally emitted energy from a patch antenna and converts it to DC power by a rectifying circuit. The system is associated with a metallic reflector which is placed behind the human body enhancing the reception. The rectifying circuit efficiency and the total system's efficiency are determined for different external antenna to human body distances and various embedded depths with or without the reflector. Experimental results, obtained in a realistic environment, validate the predicted performance and provide an initial evaluation of the transmission link. Porcine tissue and bovine tissue are both used during the measurements and results are compared against simulations.

INDEX TERMS Industrial, scientific and medical (ISM) bands, rectenna, rectifying efficiency, wireless power transmission system.

I. INTRODUCTION

Wireless energy transmission has gained significant attention in biomedical domain in recent years. An implantable medical device (IMD) could have various implementations including among others condition monitoring, drug delivery, information exchange [1]. In comparison with near-field inductive charging, far-field radiative (or microwave) charging can be used with a higher implantable depth and is much more robust to antenna location changes, orientations and surrounding environment. Furthermore, since it operates at high frequencies, the supporting antennas can be small and the implanted devices miniaturized. Thus, they can be implanted deeply inside the human body without affecting patients' comfort. Patients can also have more freedom while device charging, since relative position between the charger and the implanted antenna is not as important as in inductive charging. Finally, due to the strict limits in the power density regulation for the power emitter, RF power transmission is much safer than inductive charging.

A Radio Frequency (RF) medical energy transmission system normally consists of two parts: an antenna for capturing energy and a circuit for converting alternating current (AC) power to direct current (DC) power. There are many scientific publications on the antenna design [2], [3] and the efficiency of the microwave transmission link [2], [4]–[7].

The associate editor coordinating the review of this manuscript and approving it for publication was Abdul Halim Miah.

Moreover, the rectenna system has been also studied by many research teams in the world: For example, in [8], an equivalent global circuit simulation of a rectenna was proposed. H. W. Cheng *et al.* have studied in [9] a rectenna system that operates at 400MHz with an unrealistic circuit input power of 10dBm and rectifying efficiency of 76%. In reality, in such systems, available power is of the order of −20dBm. Indeed, most of the researchers focus on such power levels. For example, B. J. DeLong *et al.* are proposing a rectenna structure that operates at 2.4GHz in free space, but the efficiency at −20dBm is only around 7% [10]. Also, C. Liu *et al.* have worked on a rectenna system which is implanted in body that only has an efficiency of 20% with an input power of −20dBm and implantation depth of 4mm [11].

It is expected that an implanted rectenna system is efficient at low power levels. In [12], a free space compact rectenna system for ambient energy harvesting is proposed. However, the introduced system is not dedicated to biomedical applications. As for implanted rectenna systems, D. Vasisht *et al.* have studied the back-scattering method for communication and localization, in which signal reflection, attenuation, phase change and refraction are discussed [13]. X. Fang *et al.* propose a system working at Ultra High Band (UHB, 3.1- 5.1GHz). However, at this frequency region, losses could be very high even with a small implantation depth (−42dB at 18mm) [14]. Recent wireless power transfer rectenna systems have been investigated at 2.45GHz or various other frequencies in the GHz range but with a total footprint larger
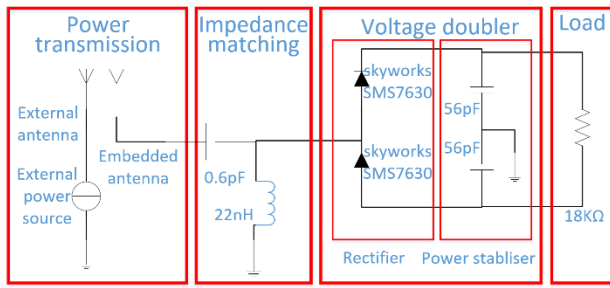
FIGURE 1. Rectenna system topology and elements used.

than 5cm^2. In conclusion, due to its high operating frequencies and low input power level, the design of a miniaturized deep-implanted and efficient energy transmitting rectenna remains a challenge for researchers [2].

In [15], the authors presented a wireless power transmission implantable rectenna system. An external half-wavelength dipole was used as a power emitter. For an embedded depth of 10mm and skin to external dipole distance equal to 175mm, the power received by the implanted antenna was around −20dBm.

In this work, we introduce a novel design of a deep-implanted practical rectenna system. The power transmission link is enhanced by an additional external metallic reflector and an improved design of the embedded antenna is detailed to avoid instability issues. Following a realistic approach, a patch antenna that resonates at the operating frequency is chosen as the emitter and the complete transmission scenario with the presence of the enhancing reflector is evaluated. A global co-simulation involving both the transmission part and the rectifying part is performed. The system is analyzed in a 3D realistic simulation environment: the entire rectenna system is embedded in a three-layer (skin, muscle and bone) cylindrical human arm model. Numerical and experimental results are presented and discussed in detail.

This paper explores a complete scenario of a wireless power transmission system including the power reception antenna and the rectifier. In comparison with work in [11], we combine all the parts comprising the two antennas and the rectifier while we analyze the transmission capabilities and the power availability. Changes in the initially presented designs are also applied for reliability and better adaptability. In addition, a metallic reflector behind the human arm is proposed, for the first time, enhancing the power transmission efficiency. Results are experimentally validated.

II. RECTIFYING SYSTEM DESIGN
A. GLOBAL SYSTEM STRUCTURE
Figure 1 shows the rectifying system including all the components and their values. The system has four parts. The first part refers to power transmission and is presented in the next section: an external rectangular patch antenna transmits the microwave power to a circular dual-band antenna which is embedded in body and resonates at 402MHz and 915MHz. Higher frequencies are not used because of increased losses inside the human tissues. As mentioned in [16], the external
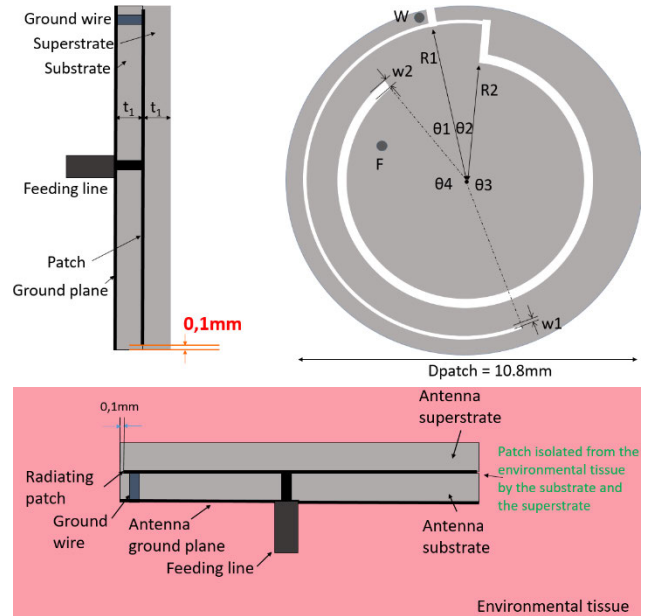

FIGURE 2. Detailed design of the reception antenna.

patch antenna operates at 902.8-928MHz. The second part deals with the impedance matching circuit, minimizing the mismatch loss and reducing the reflections. Ideal values are firstly calculated for the components. More accurate calculations are carried out when the entire printed circuit is obtained. The third part refers to designing a standard voltage doubler using the SMS 7630 Schottky diode fabricated by the Skyworks company combined with two capacitors of 56pF.

The final part is the supported device emulator which is a 18KΩ load here. Certainly, the real load could considerably variate depending on the kind and number of supported electronic devices. Authors have chosen an optimum load value for which the rectifying efficiency is maximized. From our calculations, the efficiency can variate from 27% to 31% when load takes values in the 5KΩ - 25KΩ range. A detailed discussion dedicated to the rectifier design is provided in [17].

B. RECEIVING ANTENNA DESIGN
The implanted antenna is a circular antenna. The detailed design is shown in Figure 2.

The antenna is made up of a radiating slot patch with a ground plane. Initial design of the antenna was introduced in [15]. The radiating metallic patch had the same size as the substrate and the superstrate so that it would touch the surrounding tissue. This allowed for better matching to the feeding. However, the direct contact between the radiating patch and the surrounding tissue environment could lead to instability due to the impedance variations and also reduce the gain. Thus, the patch has been redesigned with 0.1mm smaller radius than the equivalent ones of substrate and superstrate. Therefore, the patch is encapsulated by the dielectric material and it is never in contact with the lossy tissue. It is noted that the ground plane is equal in size with the substrate. The patch is grounded by a wire of radius = 0.15mm, located at point W (see Figure 3). Two circular slots are cut away from the
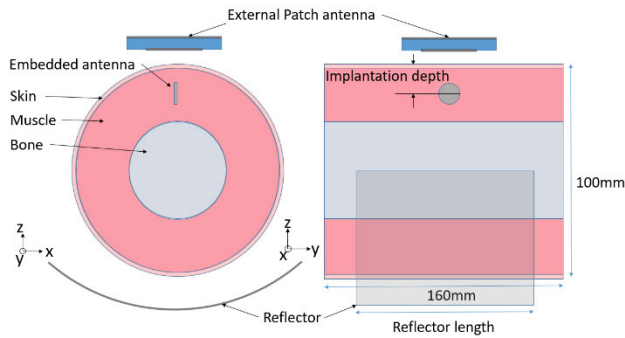
FIGURE 3. Power transmission link design.

TABLE 1. Antenna parameters.

Parameter Name	Value (mm)	Parameter Name	Value (deg)
R1	4.82	θ1	22
R2	3.7	θ2	18
w1	0.15	θ3	141
w2	0.32	θ4	179
t1	0.64		
Dpatch	10.8		
Dground	11		

patch. The patch is printed on a layer of Rogers RO 3210 ($\varepsilon_r = 10.2$, $\tan\delta = 0.003$) substrate which has a thickness of $t_1 = 0.64$ mm. The antenna is fed by a coaxial cable at point F and the patch is covered by a circular superstrate which uses the same material and has the same size as the substrate. All parameters are presented in Table 1.

It is worth pointing out that the feeding port is designed as 110Ω instead of the standard 50Ω in order to optimize the reflection coefficient at both frequencies. Since the proposed antenna is coupled to a matching circuit connected to an upconverter, the input impedance can take arbitrary values. Extensive simulations have shown optimum behavior for 110Ohm input impedance.

C. POWER TRANSMISSION LINK DESIGN

Power transmission scenario is presented in Figure 3. A three-layer cylindrical human arm model (radius: Bone 25mm; Muscle 47.5mm; Skin 50mm, see Table 3 for Dielectric Properties) is employed. In order to save calculation time, the length of the arm model is set to the minimum value so that it does not affect the results. An external rectangular patch antenna represents the emitter. A metallic wave reflector is placed behind the human arm model in order to enhance the implanted antenna's power reception. The implanted antenna is embedded along the direction of the muscle fiber in order not to hamper the arm's movement and to have a better gain with the presence of the reflector. The half-cylindrical reflector (length = 380mm, open angle = 180°, thickness = 1.2mm) is placed at 5mm distance (taking into account clothes thickness) from skin surface (see Figure 3) at the opposite to the patch antenna side. The open angle value is optimized for maximizing the enhancing effect. The reflector is made of copper and has a thickness larger than the penetration depth. For simplification and robustness, the reflector

is cylindrical instead of elliptical and its radius is chosen according to the following formula [18]:

$$f = \frac{d}{4}\cot(\frac{\theta_0}{2}) \tag{1}$$

where f is the reflector's focal distance, d is the reflector's width and θ_0 is half value of the reflector's open angle.

This system operates at 915MHz (ISM / Industrial, Scientific, and Medical band).

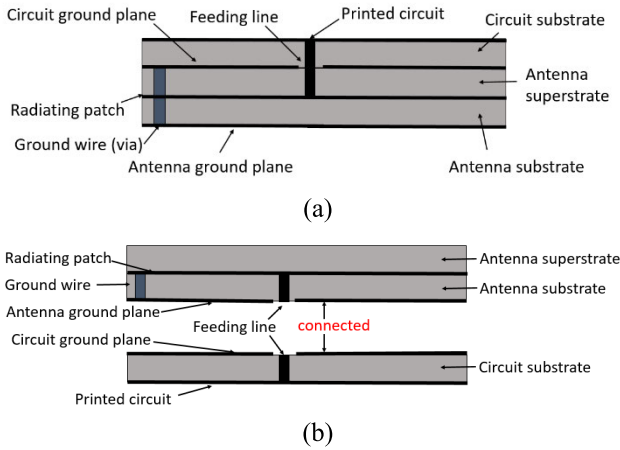### D. RECTIFYING CIRCUIT DESIGN

Once the power transmission model is established, the choice of the non-linear component for the rectifying circuit is of vital importance. The chosen diode must be adapted to high frequency and have low power consumption. The Schottky diode SMS 7630 fabricated by Skyworks company has good low-power performance. By using circuit simulation, it is shown that SMS 7630 has better rectifying efficiency than HSMS 2850 diode which has been extensively used in the past. Thus, it is chosen.

Furthermore, a matching circuit between the embedded antenna and the rest of circuit is optimized to reduce the reflection loss and the power consumption of the components. The element values are initially obtained from simulations. Then off-the-shelf components are employed. As mentioned in section II B, the feeding port of the antenna should be normalized to 110Ω. Hence, the rectifying circuit is also designed to match this value. Also, in order to satisfy the patient comfort constraint, the entire rectenna has to take as less space as possible. Since the embedded antenna radiates at broadside, the rectifying circuit could be placed at top or bottom side of the antenna. Therefore, two designs, as shown in Figure 4, are proposed in this paper. In each design, the circuit is printed on the same material as the antenna substrate. The connections are all vias (radius = 0.15mm) in order to electrically connect ground planes together.

In the first design (see Fig. 4a), a feeding line penetrates the antenna superstrate in order to connect the antenna feeding point with the circuit feeding. The antenna's ground plane, the circuit's ground plane and grounded point on the patch are all connected through a single via. In the second design (see Fig. 4b), antenna's ground plane and circuit's ground plane are electrically connected and the circuit's feeding point is connected with the patch by a feeding line. Both solutions are technically feasible. Since the antenna is electrically very small, it behaves like a dipole. As shown in section III, the antenna radiates towards its lateral direction. This presents us with the possibility of combining the rectifier at top side or bottom side to the antenna. The two ways are thus all theoretically possible. However, due to the considerations of feasibility and complexity, the second combination is employed here.

Due to dimension constraints, the circuit patterns need to fit in the small size of the substrate. A design of the circuit is shown in Figure 5, with all the components mentioned above.

The parameters values are adjusted to the parasitic capacities and edge effect that are generated from the circuit pattern

FIGURE 4. The structure of the rectenna. Two alternate and feasible positions for rectifying circuit are provided. Either at the top of the radiating patch (a) or below the ground plane (b).
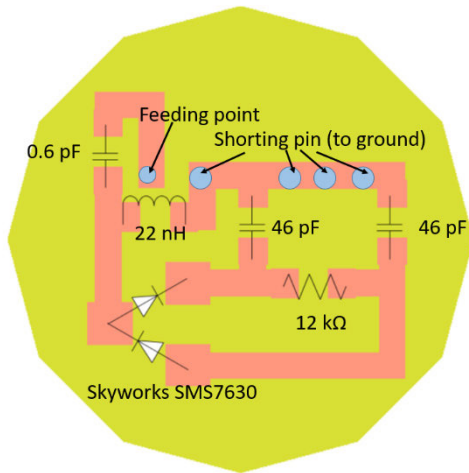
FIGURE 5. Rectifying circuit pattern with all components and their values.

by integrating the electromagnetic model of the circuit into the electromagnetic simulation.

III. NUMERICAL RESULTS

The global simulation is performed with CST [19] for electromagnetic modeling and ADS [20] for circuit simulations.

A. ANTENNA SIMULATION RESULTS

As a key factor, the reflection coefficient describes the global characteristics of the antenna. Figure 6 shows the S11 of this antenna with an input port impedance of 110Ω for various implantation depths.

As seen in Figure 6, the antenna has two distinct resonant frequencies at around 402MHz and 915MHz where S11 has values below −10dB. The resonant frequencies are almost independent on the implantation depth.

Meanwhile, since the antenna will be utilized as energy receiver, its radiation pattern and gain in the human tissue model and for different implantation depths are also important for achieving the most optimized performance. The realized gain at different depths with and without the presence of
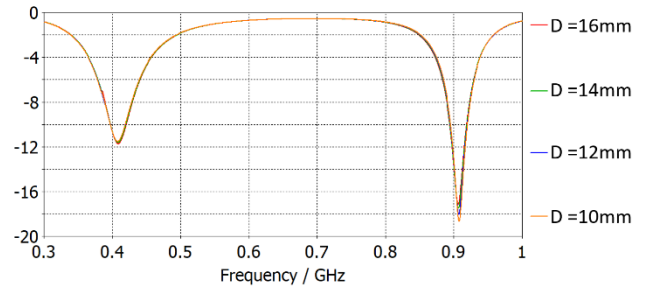
FIGURE 6. Reflection coefficient of the implanted antenna for various depths in the arm tissue model.
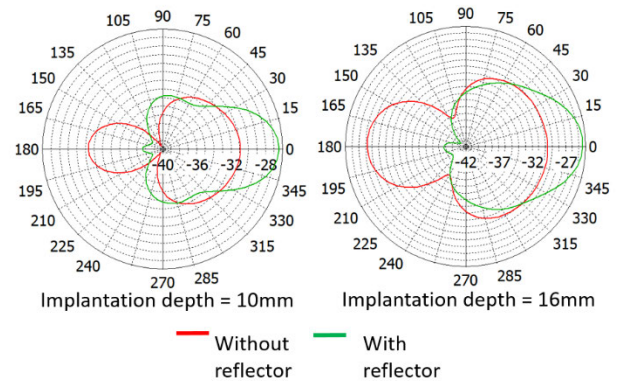
FIGURE 7. 2D horizontal radiation pattern of the antenna for different implantation depths (with and without reflector).

the reflector for the 915MHz energy transmission frequency band and at horizontal plane is given in Figure 7. As shown, the gain of the embedded antenna is around −29.8dB without reflector and −23.2dB with reflector at 16mm implantation depth while at 10mm implantation depth, it is −30.9dB without reflector and −26.5dB with reflector respectively.

B. LINK BUDGET SIMULATION RESULTS

This antenna is designed to realize energy transmission and information exchange, so it is necessary to evaluate its ability to receive energy and examine its performances for a realistic case. Due to the huge gap between the authorized emission power at MedRadio and ISM bands (−16dBm and 30dBm respectively) [21], [22], the 902.8-928MHz ISM band is chosen as the energy transmission band. Higher frequencies are not used because of increased losses inside the human tissues. Figure 3 shows the schematic model of the energy transmission case.

The transmission distance is defined as the distance between the external antenna's radiating patch and skin surface. In order to enhance the transmission, a metallic reflector is placed behind the human tissue to reflect wave to the implant. In the results below, the transmission distance is fixed at 400mm. Figure 8 show the S21 figures versus frequency at implantation depths from 10mm to 16mm.

As seen, S21 values are nearly immune to the implantation depth. This may be an advantage for patients since it is not an easy task to control accurately the embedded depth during a chirurgical operation.
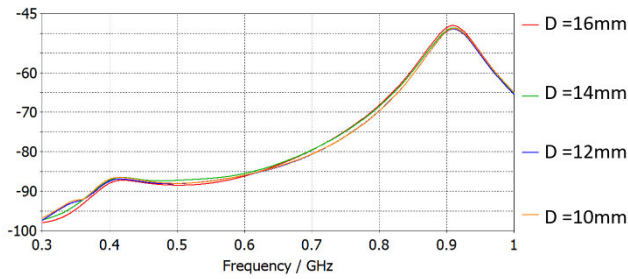
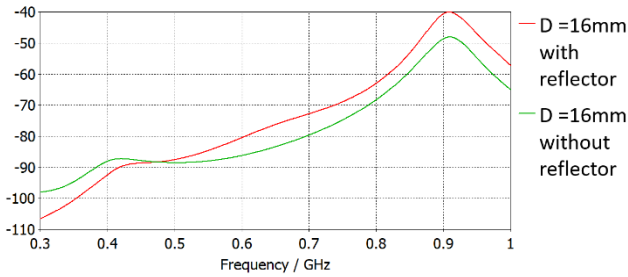**FIGURE 8.** S21 for different implantation depths.

FIGURE 9. S21 for 16mm implantation depth and 400mm transmission ditance of the external antenn with and without the reflector.
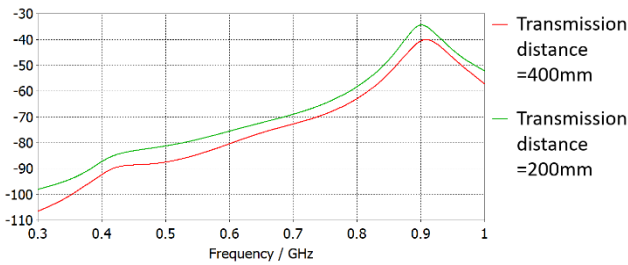

FIGURE 10. S21 for different tranmission distances at 16mm implantation depth when reflector is used.

Figure 9 shows the S21 value with and without the presence of the reflector. The presence of reflector improves S21 by 8 dB (−40.7 dB against −48.7 dB) at 16mm implantation depth and 400mm transmission distance. As compared to the maximum gain enhancement of 6.8dB when the reflector is added, the even higher enhancement of S21 is justified by the beam narrowing that the cylindrical shape reflector achieves. Indeed, the reflector not only adds to the gain of the implanted antenna, but it also acts as a focus lens for the power reception of the external – internal antenna link.

For other transmission distances and at 16mm implantation depth, the S21 maximum value at 200mm is around −34.9dB as compared to −40.7dB of 400mm transmission distance (see Figure 10). Table 2 contains all the SAR value of previous transmission scenarios when implantation depth is 16mm. According to [23], [24], those values are all in the safe range.

C. GLOBAL SYSTEM SIMULATION RESULTS

The circuit simulation is based on the electromagnetic modelling of the circuit and components available in ADS library. Antenna's simulated performance is also integrated in

TABLE 2. SAR values for different scenarios.

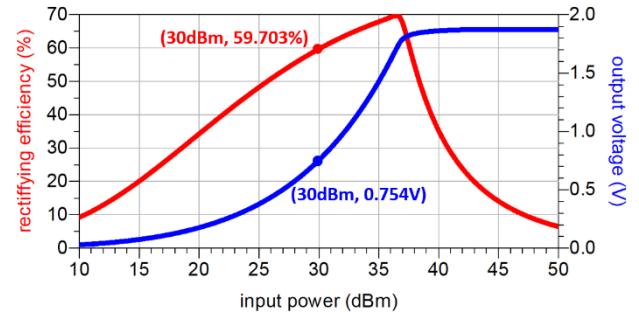|	Transmission distance	1g-average	10g-average
With reflector	200mm	0.36W/kg	0.26W/kg
	400mm	0.11W/kg	0.08W/kg
Without reflector	400mm	0.02W/kg	0.02W/kg

FIGURE 11. Global system effciency and output voltage when external patch is at 400mm far (rectifying efficiency = 59.703%, output voltage = 0.754V with 30dBm input power at the patch and for 10KΩ load).
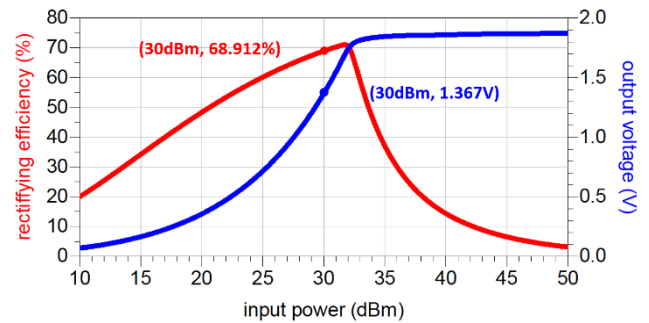

FIGURE 12. Global system effciency and output voltage when external patch is at 200mm far (rectifying efficiency = 68.912%, output voltage = 1.367V with 30dBm input power at the patch and for 8KΩ load).

ADS model. As mentioned in [22], the maximum allowable fed power to an antenna at 915MHz band is 30dBm. Simulation results for the global rectenna system are shown in Figures 11 and 12, in which the relationship between the rectifying efficiency, output voltage and input power into the external antenna is presented for various transmission distances. In this simulation, mismatch losses between antenna and circuit are also taken into account.

When the external patch antenna is fed by 30dBm power and radiates from 400mm away (transmission distance), the rectifying efficiency of the circuit is 59.7%. The value of load is chosen in order to maximize the power transmitting efficiency. The DC voltage at the load is 0.754V and the power consumed by the load is 56.9μW at this distance.

When the patch antenna is only 200mm away (transmission distance) from the patch, the rectifying efficiency of the circuit is increased to 68.912% due to the increase of the power received by the implanted antenna. The output voltage at load is 1.367V and the final rectified DC power is 233.6μW.
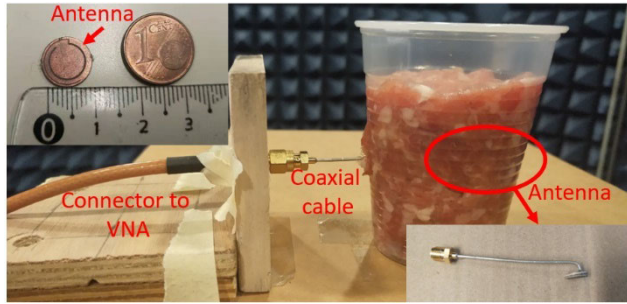
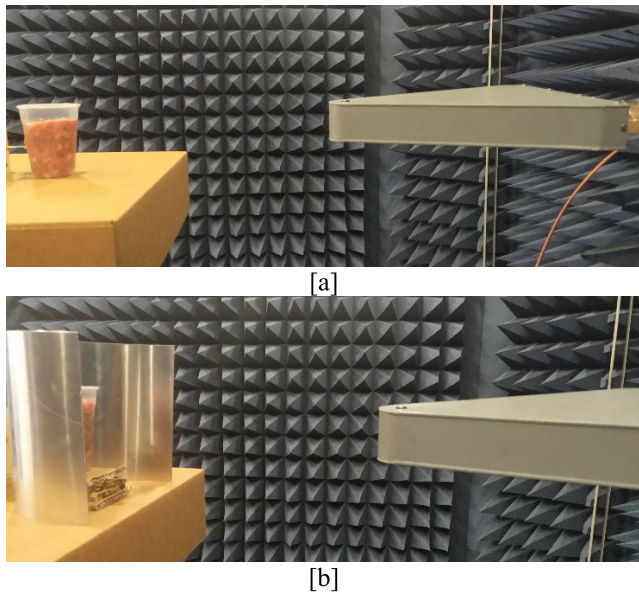**FIGURE 13.** Experiment antenna model (porcine meat).

[a]

[b]

FIGURE 14. Experiment transmission model (porcine meat), [a] without reflector [b] with reflector (not real transmission distance).

IV. EXPERIMENTAL RESULTS

A. EXPERIMENTAL SETUP

For this kind of experiments, animal tissues are preferred because of the similarity of their electromagnetic properties to human tissues [25]. In this paper, two type of tissues are tested as measurement environment for the implanted antenna: ground porcine meat and ground bovine meat. Figure13 and Fig 14 show the experimental model for the porcine meat. The experimental setup is built in an anechoic chamber ($7.2 \times 10 \times 5.8$ m^3).

In Figure13, the antenna is embedded into a cup of minced pork. The plastic cup whose thickness is negligible is used to maintain the cylindrical shape of the porcine tissue. The antenna is fed by a coaxial cable which is folded behind the antenna in order to minimize the radiating effect (see Figure 13). Then the coaxial cable is connected to the Vector Network Analyzer Agilent E8363b. The detailed feeding structure is shown at the right-bottom corner of Figure13. Printed antenna as compared to one-euro-cent for demonstration purposes is shown at the left-top corner.

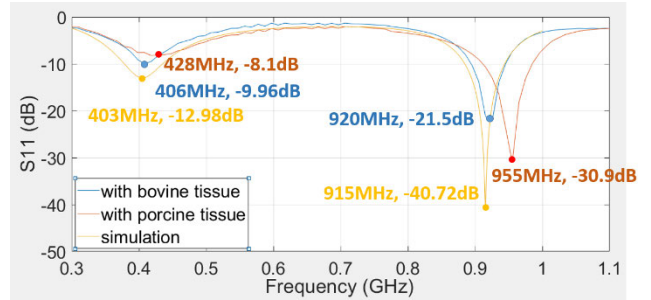The transmission model is presented in Figure14. The embedded antenna receives power from an external antenna

FIGURE 15. Antenna's measured reflection coefficient while embedded into different type of animal tissue agains simulation results.

TABLE 3. Dielectric properties of human muscle, skin and bone, bovine and ground pork tissues.

	Human muscle	Human Bone	Human Skin	Bovine Meat	Ground pork
ε_r	54.9	12.45	41.35	54	39.8
σ (S/m)	0.93	0.15	0.85	0.95	0.65

that is placed in the far field region. Furthermore, a metallic reflector is also placed behind the meat cup. It should be noted that the distance of the transmitter shown in Figure 14 is shorter than the one measured. The figure is only demonstrating the experimental setup.

B. EXPERIMENTAL RESULTS

The antenna has been designed to be implanted in the muscle layer. The ground pork meat has 20% to 30% of fat inside. The ground beef meat used has less than 5% of fat inside. It is noted that ground pork meat has a lower permittivity than lean meat because of fat presence. Subsequently, the antenna's resonant frequencies shift to higher values (than the corresponding ones in simulations). Figure 15 shows the antenna's measured reflection coefficient when is embedded into porcine tissue and bovine tissue against simulation results.

As seen, the antenna's resonant frequencies when implanted into bovine tissues (5% fat) slightly shift to higher values. The shifting may be caused by two possible reasons: the 5% fat in the tissue and random air bubbles that exist among the tissue. Both factors will decrease the permittivity of the environment and alter the resonant frequency of the antenna. A comparison between human tissues, ground pork and bovine meat is provided in Table 3 as follows [26]–[28]:

Generally, in measurements, porcine ground meat with fat is usually considered to represent the human tissue thanks to its availability and its similarity to dielectric properties of human tissues [25]. In simulations, a homogenous human muscle is used as embedding environment. Therefore, when the bovine tissue (with less fat) is used, results are closer to the simulated ones. Nevertheless, in real life, people with only 5% of fat is a relatively rare case, so the results using the ground pork should be closer to the reality.

Due to this probable frequency shifting, it is necessary to study the performance of the rectifying circuit under different frequencies in case of minor frequency shifting.
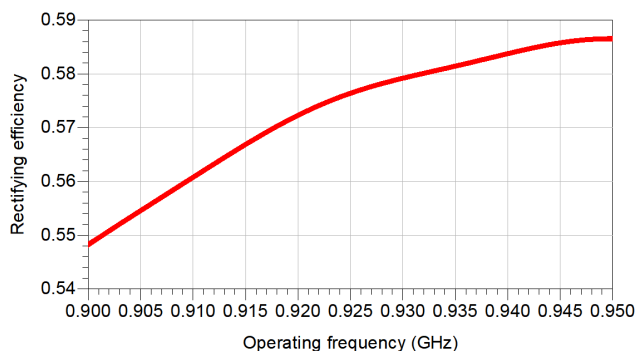
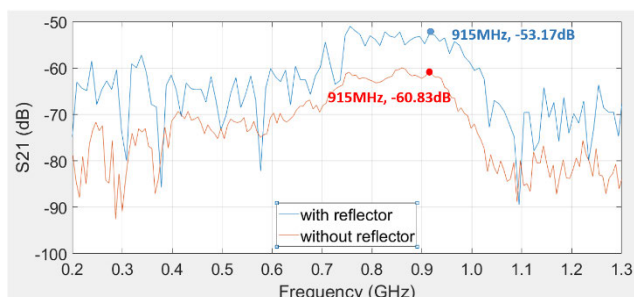**FIGURE 16.** Rectifier efficiency for the 900-950MHz frequency range.

FIGURE 17. Experiment transmission results (bovine tissue).

The performance of the rectifier at 900MHz to 950MHz with −11dBm input power to the circuit is thus analyzed in simulations and shown in the following Figure 16. As observed, the rectifying efficiency changes slightly for various operating frequencies. For circuits' input power from −10dBm to −20dBm, this change is no higher than 4%.

Since the bovine tissue has less fat and is more similar to human muscle environment, it is used for the rest of the measurement. The external antenna is a log periodic antenna ESLP 9145 from Schwarzbeck company. Due to the tiny size, the far field size of the implanted antenna is much smaller than the external one. The length of the external antenna is 50cm. It has a gain of around 6dBi and is linearly polarized. According to the definition of the Fresnel distance, the far field distance for this antenna is around 1.5m.

Figure 17 shows the measured S21 parameters with and without the presence of the metallic reflector for a transmission distance of 1.5m. As seen, the S21 could be enhanced by around 7dB with the presence of the reflector, which validates the simulation results.

The experimental process and results regarding the rectifying circuit are presented in [17].

V. CONCLUSION

A miniaturized wireless RF to DC implantable power rectifying system for biomedical applications is presented in this paper. The system operates at 915 MHz ISM band supported by a dual band miniaturized circular antenna. A metallic reflector is considered for enhancing the power reception. Realistic scenarios are investigated. Experimental results obtained in an anechoic chamber are analyzed and validate the efficiency of the transmission link.

Implantable Medical Devices are used in various cases in the biomedical domain. Compared to a nearfield wireless energy transmission which is more often used for rather large devices like pacemakers, the power transmission system proposed in this paper occupies less space and should be thus used in supporting miniature sensors. It has been discussed and shown in [17] that such a system can support small sensors which require low energy and low voltage to operate [29]–[31].

In future work, the combined antenna-circuit system will be fabricated and measured in order to evaluate the global power transmission efficiency.

REFERENCES

[1] K. S. Nikita, *Handbook of Biomedical Telemetry*. Hoboken, NJ, USA: Wiley, 2013.

[2] S. Bakogianni and S. Koulouridis, "A dual-band implantable Rectenna for wireless data and power support at sub-GHz region," *IEEE Trans. Antennas Propag.*, vol. 67, no. 11, pp. 6800–6810, Nov. 2019.

[3] A. Kiourti and K. S. Nikita, "Miniature scalp-implantable antennas for telemetry in the MICS and ISM bands: Design, safety considerations and link budget analysis," *IEEE Trans. Antennas Propag.*, vol. 60, no. 8, pp. 3568–3575, Aug. 2012.

[4] R. Li and S. Xiao, "Compact slotted semi-circular antenna for implantable medical devices," *Electron. Lett.*, vol. 50, no. 23, pp. 1675–1677, Nov. 2014.

[5] Z. Chen, H. Sun, and W. Geyi, "Maximum wireless power transfer to the implantable device in the radiative near field," *IEEE Antennas Wireless Propag. Lett.*, vol. 16, pp. 1780–1783, 2017.

[6] C. J. Sanchez-Fernandez, O. Quevedo-Teruel, J. Requena-Carrion, L. Inclan-Sanchez, and E. Rajo-Iglesias, "Dual-band microstrip patch antenna based on short-circuited ring and spiral resonators for implantable medical devices," *IET, Microw. Antennas Propag.*, vol. 4, no. 8, pp. 1048–1055, 2010.

[7] H. Zhang, S.-P. Gao, T. Ngo, W. Wu, and Y.-X. Guo, "Wireless power transfer antenna alignment using intermodulation for two-tone powered implantable medical devices," *IEEE Trans. Microw. Theory Techn.*, vol. 67, no. 5, pp. 1708–1716, May 2019.

[8] B. Essakhi, G. Akoun, and L. Pichon, "A global time domain circuit simulation of a microwave rectenna," *Int. J. Numer. Model., Electron. Netw., Devices Fields*, vol. 20, nos. 1–2, pp. 3–15, Jan. 2007.

[9] H.-W. Cheng, T.-C. Yu, and C.-H. Luo, "Direct current driving impedance matching method for rectenna using medical implant communication service band for wireless battery charging," *IET Microw., Antennas Propag.*, vol. 7, no. 4, pp. 277–282, Mar. 2013.

[10] B. J. DeLong, A. Kiourti, and J. L. Volakis, "A radiating near-field patch rectenna for wireless power transfer to medical implants at 2.4 GHz," *IEEE J. Electromagn., RF Microw. Med. Biol.*, vol. 2, no. 1, pp. 64–69, Mar. 2018.

[11] C. Liu, Y.-X. Guo, H. Sun, and S. Xiao, "Design and safety considerations of an implantable rectenna for far-field wireless power transfer," *IEEE Trans. Antennas Propag.*, vol. 62, no. 11, pp. 5798–5806, Nov. 2014.

[12] A. Okba, A. Takacs, and H. Aubert, "Compact rectennas for ultra-low-power wireless transmission applications," *IEEE Trans. Microw. Theory Techn.*, vol. 67, no. 5, pp. 1697–1707, May 2019.

[13] D. Vasisht, G. Zhang, O. Abari, H.-M. Lu, J. Flanz, and D. Katabi, "In-body backscatter communication and localization," in *Proc. Conf. ACM Special Interest Group Data Commun.*, Aug. 2018, pp. 132–146.

[14] X. Fang, M. Ramzan, Q. Zhang, S. Perez-Simbor, Q. Wang, N. Neumann, C. Garcia-Pardo, N. Cardona, and D. Plettemeier, "Experimental in-body to on-body and in-body to in-body path loss models of planar elliptical ring implanted antenna in the ultra-wide band," in *Proc. 13th Int. Symp. Med. Inf. Commun. Technol. (ISMICT)*, Oslo, Norway, May 2019, pp. 1–5.

[15] S. Ding, S. Koulouridis, and L. Pichon, "Implantable rectenna system for biomedical wireless applications," in *Proc. IEEE Wireless Power Transf. Conf. (WPTC)*, London, U.K., Jun. 2019, pp. 1–4.

[16] S. Ding, S. Koulouridis, and L. Pichon, "A dual-band miniaturized circular antenna for deep in body biomedical wireless applications," in *Proc. 13th Eur. Conf. Antennas Propag. (EuCAP)*, Krakow, Poland, 2019, pp. 1–4.

[17] S. Ding, S. Koulouridis, and L. Pichon, "Miniaturized implantable power transmission system for biomedical wireless applications," *Wireless Power Transf.*, vol. 7, no. 1, pp. 1–9, Mar. 2020.

[18] Constantine A. Balanis, *Antenna Theory*. Hoboken, NJ, USA: Wiley, 1982.

[19] *Computer Simulation Technology (CST) STUDIO SUITE. Version 2017*, Dassault Systèmes Simulia Corp, Johnston, RI, USA. [Online]. Available: http://www.cst.com

[20] *Advanced Design System (ADS)*, Keysight Technology, Santa Rosa, CA, USA, 2019.

[21] *International Telecommunications Union*, document Recommendation ITU-R RS.1346, 1998.

[22] *Standard Specification for Radiated Emission Limits, General Requirements*, document FCC 15, 2009.

[23] *IEEE Standard for Safety Levels With Respect to Human Exposure to Radiofrequency Electromagnetic Fields, 3 kHz to 300 GHz*, IEEE Standard C95.1, 1999.

[24] *IEEE Standard for Safety Levels With Respect to Human Exposure to Radiofrequency Electromagnetic Fields, 3 kHz to 300 GHz*, IEEE Standard C95.1, 2005.

[25] M. Vallejo, J. Recas, P. del Valle, and J. Ayala, "Accurate human tissue characterization for energy-efficient wireless on-body communications," *Sensors*, vol. 13, no. 6, pp. 7546–7569, Jun. 2013.

[26] S. Gabriel, R. W. Lau, and C. Gabriel, "The dielectric properties of biological tissues: II. Measurements in the frequency range 10 hz to 20 GHz," *Phys. Med. Biol.*, vol. 41, no. 11, pp. 2251–2269, Nov. 1996.

[27] Z. A. Deneris, D. E. Pe'a, and C. M. Furse, "A layered pork model for subdermal antenna tests at 433 MHz," *IEEE J. Electromagn., RF Microw. Med. Biol.*, vol. 3, no. 3, pp. 171–176, Sep. 2019.

[28] L. Abdilla, C. Sammut, and L. Z. Mangion, "Dielectric properties of muscle and liver from 500 MHz–40 GHz," *Electromagn. Biol. Med.*, vol. 32, no. 2, pp. 244–252, Jun. 2013.

[29] N. T. Trung and P. Häfliger, "A submicrowatt implantable capacitive sensor system for biomedical applications," *IEEE Trans. Circuits Syst. II, Exp. Briefs*, vol. 62, no. 2, pp. 209–213, Feb. 2015.

[30] H. Danneels, K. Coddens, and G. Gielen, "A fully-digital, 0.3 V, 270 nW capacitive sensor interface without external references," in *Proc. ESSCIRC*, Sep. 2011, pp. 287–290.

[31] W. Bracke, P. Merken, R. Puers, and C. Van Hoof, "Ultra-low-power interface chip for autonomous capacitive sensor systems," *IEEE Trans. Circuits Syst. I, Reg. Papers*, vol. 54, no. 1, pp. 130–140, Jan. 2007.

[32] Z. Tan, R. Daamen, A. Humbert, K. Souri, Y. Chae, Y. V. Ponomarev, and M. A. P. Pertijs, "A 1.8 V 11 μW CMOS smart humidity sensor for RFID sensing applications," in *Proc. IEEE Asian Solid-State Circuits Conf.*, Nov. 2011, pp. 105–108.

[33] M. Kamarainen, M. Paavola, M. Saukoski, E. Laulainen, L. Koskinen, M. Kosunen, and K. Halonen, "A 1.5 μW 1V 2nd-order $\Delta\Sigma$ sensor front-end with signal boosting and offset compensation for a capacitive 3-axis micro-accelerometer," in *IEEE Int. Solid-State Circuits Conf. Dig. Tech. Papers*, San Francisco, CA, USA, Feb. 2008, pp. 578–637.

SHUOLIANG DING was born in Shenyang, China, in 1994. He received the Diploma Engineer degree from the Ecole Centrale de Nantes in France and the Diploma master's degree from Beihang University, Beijing, China in 2017. He is currently pursuing the Ph.D. degree with the CentraleSupelec, Paris, France.

In 2017, he joined the Group of Electrical Engineering in Paris (GeePs). During his Ph.D. study, he has authored several papers in international conferences. His current research interests include bio-electromagnetics, antenna theory, implantable antenna design, and wireless powering devices for biomedical applications.

STAVROS KOULOURIDIS was born in Athens, Greece, in 1975. He received the Diploma Engineer degree in electrical and computer engineering and the Ph.D. degree in microwave engineering from the National Technical University of Athens, Greece, in 1999 and 2003, respectively.

From 1999 to 2003 he worked as a Research Engineer with the Microwave and Fiber Optics Laboratory, and the Biomedical Simulations and Imaging Unit, National Technical University of Athens. He taught several classes at the School of Pedagogic and Technological Education (ASPAITE), from 2000 to 2003. He was also a Teaching Assistant with the National Technical University of Athens, from 2000 to 2002. From 2004 to 2008, he worked as Postdoctoral Researcher with the Electroscience Laboratory, The Ohio State University, Columbus, OH, USA. In March 2009, he joined the Electrical and Computer Engineering Department, University of Patras, Greece. Since August 2013, he has been an Assistant Professor position. From 2015 to 2016, he was Visiting Professor with the Group of Electrical Engineering–Paris (GeePs) / CNRS-CentraleSupelec, University Paris-Sud, Université Paris-Saclay, Sorbonne Université. He also leads the Microwave Communications Group. He has published more than 80 refereed journals and conference proceeding papers. His research interests include antenna and microwave devices design, development and fabrication of novel materials, microwave applications in medicine, electromagnetic optimization techniques, and applied computational electromagnetics.

Dr. Koulouridis was a recipient of a three year Ph.D. Scholarship on Biomedical Engineering from the Hellenic State Scholarships Foundation in 2001. In May 2005, he received the Annual Award for the Best Dissertation from the National Technical University of Athens. He is the Chair of IEEE AP/MTT/ED Local Greek Chapter. He was the General Chair of the International Workshop in Antennas Technology (IWAT) 2017. He is serving as a Reviewer for several scientific international journals.

LIONEL PICHON received the Diploma Engineering degree from the Ecole Supérieure d'Ingénieurs en Electronique et Electrotechnique in 1984, and the Ph.D. degree in electrical engineering from the Laboratoire de Génie Electrique de Paris, in 1989. He got a position at the Centre National de la Recherche Scientifique (CNRS) in 1989. He is currently the Directeur de Recherche (Senior Research Scientist) with the Group of electrical engineering–Paris (GeePs), a laboratory belonging to four institutions: the CNRS, CentraleSupélec, Université Paris-Saclay, Sorbonne Université. He is author or coauthor of more than 120 journal articles in peer-reviewed journals. His research interests include computational electromagnetics for wave propagation, scattering, and electromagnetic compatibility. He is serving as a Reviewer for several scientific international journals. He is an Associated Editor of the *European Physical Journal–Applied Physics* (EPJ-AP).

• • •